miR-29a inhibits human retinoblastoma progression by targeting STAT3

SHU LIU[1], XIAOMENG ZHANG[1], CHUNMEI HU[2], YINGXUE WANG[3] and CHUNLING XU[1]

Departments of [1]Ophthalmology, [2]Tumor and Hematology and [3]Electrical Diagnosis, The Second Hospital of Jilin University, Changchun, Jilin 130041, P.R. China

Received July 22, 2017; Accepted December 1, 2017

DOI: 10.3892/or.2017.6144

Abstract. Retinoblastoma (RB) is the most common malignancy that occurs during childhood. Growing evidence supports a crucial role for microRNAs (miRNAs) in regulating the initiation and progression of RB. Aberrant expression of microRNA-29a (miR-29a) has been found in many types of cancers, but not including RB. Therefore, the aims of the present study were to evaluate the regulatory role and underlying mechanism of miR-29a in human RB. In the present study, we found that miR-29a expression was significantly downregulated in RB tissues and cell lines. Overexpression of miR-29a in RB cells significantly inhibited cell proliferation, migration, and invasion and promoted cell apoptosis *in vitro*. Additionally, signal transducer and activator of transcription 3 (STAT3) was identified as a direct target of miR-29a in RB cells. miR-29a overexpression in RB cells not only inhibited STAT3 expression but also altered expression of its downstream genes, including, Bcl2, cyclin D1 and matrix metalloproteinase 2 (MMP-2). *STAT3* mRNA expression was upregulated in RB tissues and negatively correlated with miR-29a expression. Reintroduction of STAT3 without 3'-untranslated region (3'UTR) reversed the inhibitory effects of miR-29a on cell proliferation, migration and invasion. *In vivo* study confirmed that overexpression of miR-29a also inhibited tumor formation of RB in a nude mouse model by repressing STAT3. Collectively, these data suggest that miR-29a exerts a tumor suppressor effect on RB by repressing STAT3, supporting the targeting of miR-29a as a potentially effective therapeutic method for RB.

Introduction

Retinoblastoma (RB) is the most common intraocular malignant tumor in childhood with a high mortality rate, especially in developing countries (1,2). Although great efforts have been made in the treatment of RB in recent years, the survival rate remains poor mainly due to limitations in the early diagnosis of the disease and the development of metastasis (3). Therefore, it is crucial to explore the key molecular mechanisms involved in RB initiation and development to identify new diagnostic markers and therapeutic targets.

MicroRNAs (miRNAs) are small (18-25 nucleotide long), non-coding RNAs that regulate gene expression via binding to the 3'-untranslated region (3'UTR) of target mRNAs, leading to mRNA degradation or translational inhibition (4,5). It has been demonstrated that miRNAs are involved in diverse biological processes, including metabolic homeostasis, cell proliferation and cell apoptosis (6,7). Accumulating evidence shows that the altered expression of miRNAs are involved in the initiation and progression of cancer (8), suggested that miRNAs can serve as diagnostic markers and therapeutic targets in human cancers. miRNAs have now been identified to serve as either tumor suppressors or as oncogenes in RB by exerting effects on important regulatory cellular pathways (9,10).

An accumulating body of evidence shows that microRNA-29a (miR-29a) expression is dysregulated and plays crucial roles in progression and development of multiple cancers (11-16). Yet, the role and underlying mechanism of miR-29a in RB cells remain unclear. The aims of the present study were to investigate miR-29a expression and clinical significance, and determine the biological function of miR-29a in RB and explore the possible regulating mechanisms in RB cells.

Materials and methods

Human tissue samples and cell lines. Twenty human RB specimens and 5 retina tissues were obtained from patients with RB and ruptured globe at the Department of Ophthalmology, the Second Hospital of Jilin University, respectively. All patients had not received preoperative radiotherapy and/or chemotherapy prior to enucleation. All tissues were stored in liquid nitrogen until RNA isolation. This study was approved by the Ethics Committee of Jilin University. Written informed consent was obtained from each patient.

Two human RB cell lines (Y79 and SO-RB50) were obtained from the Institute of Biochemistry and Cell Biology of the Chinese Academy of Sciences (Shanghai, China).

Correspondence to: Dr Chunling Xu, Department of Ophthalmology, The Second Hospital of Jilin University, 218 Zhiqiang Street, Nanguan, Changchun, Jilin 130041, P.R. China
E-mail: xucl@jlu.edu.cn

Key words: microRNAs, miR-29a, retinoblastoma, STAT3

All cells were maintained at 37˚C in a humidified 5% CO_2 atmosphere in RPMI-1640 medium (Gibco, Grand Island, NY, USA) containing 10% fetal bovine serum (FBS, Gibco), 100 U/ml penicillin, and 100 mg/ml streptomycin.

Plasmid, microRNA mimic, and transfection. Full-length STAT3 (without the 3'UTR) was amplified by PCR and inserted into the eukaryotic expression vector pcDNA3.1 (+) (Invitrogen). The STAT3 3'UTR target site for miR-29a was amplified by PCR, and subcloned into the pGL3-control vector (Ambion, Austin, TX, USA) and named WT-STAT3-3'UTR. Quick-Change Mutagenesis kit (Stratagene, Heidelberg, Germany) was used for mutagenesis of the miR-29a target-site in the STAT3 3'UTR, and was referred to as MT-STAT3-3'UTR. The miR-29a mimic or corresponding negative control (miR-NC) were chemically synthesized by GenePharma Co. (Shanghai, China). For the transfection experiments, $2x10^5$ RB cells were seeded in a 6-cm dish, and cultured in RPMI-1640 with 10% FBS up to 70-80% confluence. Then transfection was performed using Lipofectamine 2000 (Invitrogen, Carlsbad, CA, USA) according to the manufacturer's instructions.

RNA extraction and quantitative real-time PCR (qRT-PCR). Total RNA was isolated from tissue samples and cell lines by the TRIzol reagent (Invitrogen) following the manufacturer's protocol. For miR-29a expression analysis, total RNA was reverse transcribed to cDNA using the microRNA reverse transcription kit (Takara, Dalian, China), and then were quantified with SYBR miRNA detection assays (Takara) under an Applied Biosystems 7500 HT system (Thermo Fisher Scientific, Inc., Waltham, MA, USA) using primers for U6 and miR-29a (Applied Biosystems). For *STAT3* mRNA detection, total RNA was reverse transcribed to cDNA using the Prime-Script RT reagent kit (Takara), and then were quantified using SYBR Premix Ex Taq (Takara). The primers for STAT3 and glyceraldehyde 3-phosphate dehydrogenase (GAPDH) used in this study were described previously (17). U6 and GAPDH were used as control for miR-29A and *STAT3* mRNA, respectively using the $2^{-\Delta\Delta CT}$ method.

Cell proliferation, cell cycle distribution, apoptosis, migration and invasion analyses. 3-(4,5-Dimethylthiazol-2-yl)-2, 5-diphenyltetrazolium bromide (MTT) assay was performed to determine cell proliferation. Briefly, $5x10^3$ transfected cells were seeded into a 96-well plate, and cultured for 24-72 h. At the indicated time, 20 μl MTT solution (5 mg/ml, Sigma-Aldrich, St. Louis, MO, USA) was added to each well and additionally cultured for 4 h. The MTT solution was removed and 150 μl dimethyl sulfoxide (DMSO, Sigma-Aldrich) was added to each well. Optical density (OD) was detected at the wavelength of 570 using a Benchmark Plus™ microplate spectrometer (Bio-Rad, Hercules, CA, USA).

For cell cycle and apoptosis assays, the RB cells were harvested 48 h after transfection, and washed with PBS. Then $5x10^4$ cells were resuspended in 500 μl of binding buffer containing 5 μl of Annexin V-fluorescein isothiocyanate (FITC) and 5 μl of propidium iodide (PI). Cell cycle arrest was detected using FACS-Calibur™ flow cytometer (BD Biosciences, San Jose, CA, USA), and was analyzed by CellQuest software (BD Biosciences). Cell apoptosis was determined using Annexin V-FITC Apoptosis Detection kit (KeyGEN, Shanghai, China) according to the instructions of the manufacturer. The data were analyzed with FlowJo v5.7.2 software (BD Biosciences).

For cell migration, the transfected cells were seeded into 24-well dishes and cultured to near (>80%) confluence. Then an artificial homogeneous wound was created with a sterile pipette tip onto the monolayer, and cultured for 24 h. Cells were imaged using inverted Nikon Eclipse TS100 phase-contrast microscope (Tokyo, Japan) at 0 and 24 h after the wounding. Wound closure was determined using Nikon NIS-Element Basic Research v3.2 software (Tokyo, Japan).

Transwell chamber assay was performed to analyze cell invasion. Matrigel was employed to pre-coat the membrane of Transwells to simulate a matrix barrier for the invasion assay. The transfected cells growing in the log phase were seeded on the upper champers at a density of $2x10^5$ cells/well. Medium with 10% FBS was added to the lower chamber to stimulate cell invasion. After 24 h of incubation, cells which migrated to the lower chamber were fixed with paraformaldehyde for 5 min, and stained with 0.1% crystal violet for 5 min. The images of cells were photographed with a TS100 inverted microscope (Nikon) at x200 magnification, and the cell number was counted in five selected randomly fields per membrane.

miRNA target prediction and luciferase reporter assay. Three online databases for target site predictions (TargetScan7.1, PicTar and miRDB) were used to predict the putative targets of miR-29a. For the luciferase reporter assay, RB cells were cotransfected with miR-29a mimic or miR-NC and WT-STAT3-3'UTR or MT-STAT3-3'UTR reporter plasmid by Lipofectamine 2000. The cells were lysed and luciferase activities were detected 48 h after transfection using a Dual-Luciferase® Reporter Assay kit (Promega, Madison, WI, USA) according to the manufacturer's protocols. *Renilla* luciferase activity was normalized to firefly luciferase activity.

Western blotting. RB cells and tissues were harvested and lysed with RIPA buffer (Beyotime, Jiangsu, China), following by quantification with the BCA protein assay kit (Pierce, Bonn, Germany). The proteins were separated by 10% SDS-polyacrylamide gel electrophoresis, and subsequently transferred to polyvinylidene difluoride (PVDF) membranes (Merck, Millipore, Germany). The membranes were blocked with 5% nonfat milk and then incubated with the following primary antibodies overnight at 4˚C: anti-STAT3 (1:1,000, cat. no. sc-293151), anti-Bcl-2 (1:1,000, cat. no. sc-56015), anti-cyclin D1 (1:1,000, cat. no. sc-70899; all from Santa Cruz Biotechnology, Inc., Santa Cruz, CA, USA) and anti-MMP2 (1:500, cat. no. 40994; Cell Signaling Technology, Danvers, MA, USA) or anti-GAPDH (1:3,000, cat. no. sc-365062; Santa Cruz Biotechnology, Inc.). The blots were washed with PBST and incubated with horseradish peroxidase (HRP)-conjugated corresponding secondary antibody for 2 h at room temperature. Protein bands were observed using an enhanced chemiluminescence system (Thermo Fisher Scientific, Inc.) and exposed to X-ray film. GAPDH was used as a control.

Xenograft tumor model. BALB/c-nu mice (5-6 weeks of age and weighing 20-25 g) were purchased from the Experimental

Animal Center of Jilin University, and their care was in accordance with institutional guidelines. Stable cell lines with high expression of miR-29a were established by transfecting RB cells with the miR-29a mimic. Mice were inoculated subcutaneously with $2x10^6$ Y79 cells expressing miR-NC (Y79/miR-NC cells) in the left dorsal flank and $2x10^6$ Y79 cells expressing miR-29a (Y79/miR-29a cells) in the right dorsal flank. Tumor volume was determined once every week from the first injection until sacrifice according to the following formula: $V = (LxW^2/2$ (where V is the volume; L, length; W, width of tumor). On day 35 day, the mice were sacrificed, and the tumors were stripped, and the wet weight of each tumor was determined. Tumor tissues were stored at -80˚C for further analysis.

Statistical analysis. SPSS statistical software for Windows version 19 (SPSS, Chicago, IL, USA) and GraphPad Prism 5.01 (GraphPad Software, Inc, San Diego, CA, USA) software were used for statistical analysis. All data are represented as the mean ± SD (standard deviation) from at least three independent experiments. Comparisons between the groups were analyzed with two-tailed Student's t-test or one-way ANOVA. Spearman's rank correlation analysis was performed to analyze correlation between miR-29a and STAT3. A $P<0.05$ was considered to indicate a statistically significant result.

Results

miR-29a is downregulated in RB tissues and RB cell lines. To investigate the expression status of miR-29a in RB and RB cell lines, real-time RT-PCR (qRT-PCR) was conducted. Expression of miR-29a was lower in the 20 RB tissues and 2 RB cell lines than that observed in the 5 normal retinal tissues ($P<0.05$; Fig. 1), suggesting that the downregulation of miR-29a may be involved in human RB tumorigenesis.

Overexpression of miR-29a inhibits cell proliferation and promotes apoptosis in RB cells. To assess the biological effects of miR-29a on RB cells, Y79 and SO-RB50 cells were transiently transfected with miR-29a mimic and miR-NC, and then cell proliferation, cell cycle distribution and apoptosis were determined. qRT-PCR confirmed miR-29a overexpression in Y79 and SO-RB50 cells (Fig. 2A). The MTT assay showed that restoration of miR-29a expression in Y79 and SO-RB50 cells significantly inhibited cell proliferation (Fig. 2B). Since cell proliferation is closely associated with cell cycle arrest, we investigated the effect of miR-29a on the cell cycle. FACS analysis showed that transfection of the Y79 and SO-RB50 cells with the miR-29a mimic significantly increased the proportion of cells in the G0/G1 phase and reduced the proportion of S phase cells compared to the cells transfected with miR-NC (Fig. 2C). In addition, we found that restoration of miR-29a in Y79 and SO-RB50 cells significantly increased the cell apoptosis rate (Fig. 2D).

miR-29a inhibits the migration and invasion of RB cells. To study the effect of miR-29a on migration and invasion abilities, wound healing and invasion chamber assays were performed in Y79 and SO-RB50 cells transfected with miR-29a or miR-NC, respectively. It was found that restoration of miR-29a in RB cells significantly decreased migration (Fig. 3A) and invasion (Fig. 3B) capacity.

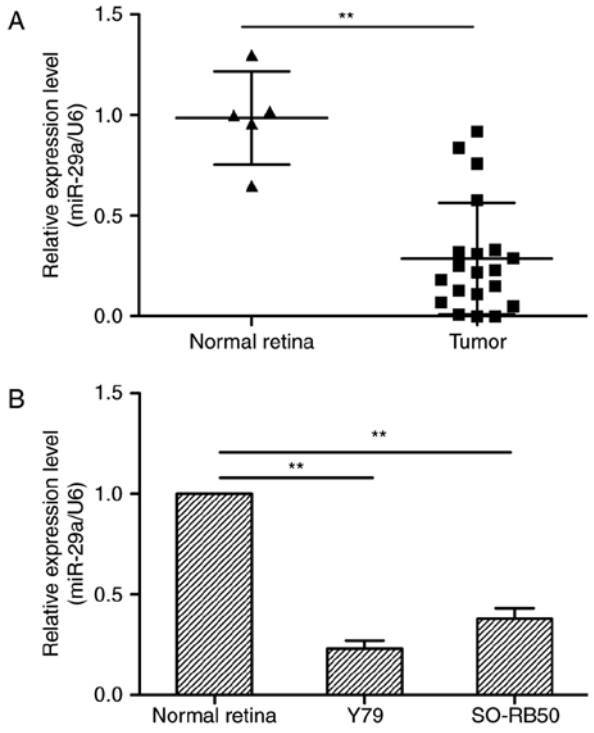

Figure 1. miR-29a expression level in primary retinoblastoma (RB) tissues and cell lines. (A) miR-29a expression levels were significantly decreased in RB tissues compared to normal retinal tissues. (B) miR-29a expression levels were downregulated in RB cell lines, when compared with normal retinal tissues. **P<0.01.

STAT3 is a direct target gene of miR-29a in RB cells. Three miRNA databases (Targetscan, Pictar and Miranda) were used to identify a putative miR-29a-binding site. Among the candidate targets, the 3'UTR of human STAT3 contains a putative region that matches to the seed sequence of miR-29a (Fig. 4A). To confirm whether miR-29a directly binds to STAT3, luciferase activity assay was performed. It was found that miR-29a overexpression markedly reduced the luciferase activity of the WT-*STAT3*-3'UTR, but not the MT-*STAT3*-3'UTR in Y79 and SO-RB50 cells (Fig. 4B). To further confirm the effect of miR-29a on STAT3 expression, we analyzed the STAT3 expression at the mRNA and protein levels in Y79 and SO-RB50 cells transfected with miR-29a mimic or miR-NC by qRT-PCR and western blot analysis, respectively. We found that the *STAT3* expression at the mRNA and protein levels was decreased in the Y79 and SO-RB50 cells transfected with miR-29a mimic compared with cells transfected with miR-NC (Fig. 4C and D). We also found that miR-29a overexpression also significantly inhibited cyclin D1, Bcl-2 and MMP-9 expression, several downstream proteins of STAT3, in the Y79 and SO-RB50 cells (Fig. 4D). These results indicate that STAT3 is a direct target of miR-29a in RB cells.

STAT3 expression is upregulated, and inversely correlated with miR-29a expression in RB tissues. Next, we detected the *STAT3* mRNA expression in the 20 RB tissues and 5 normal

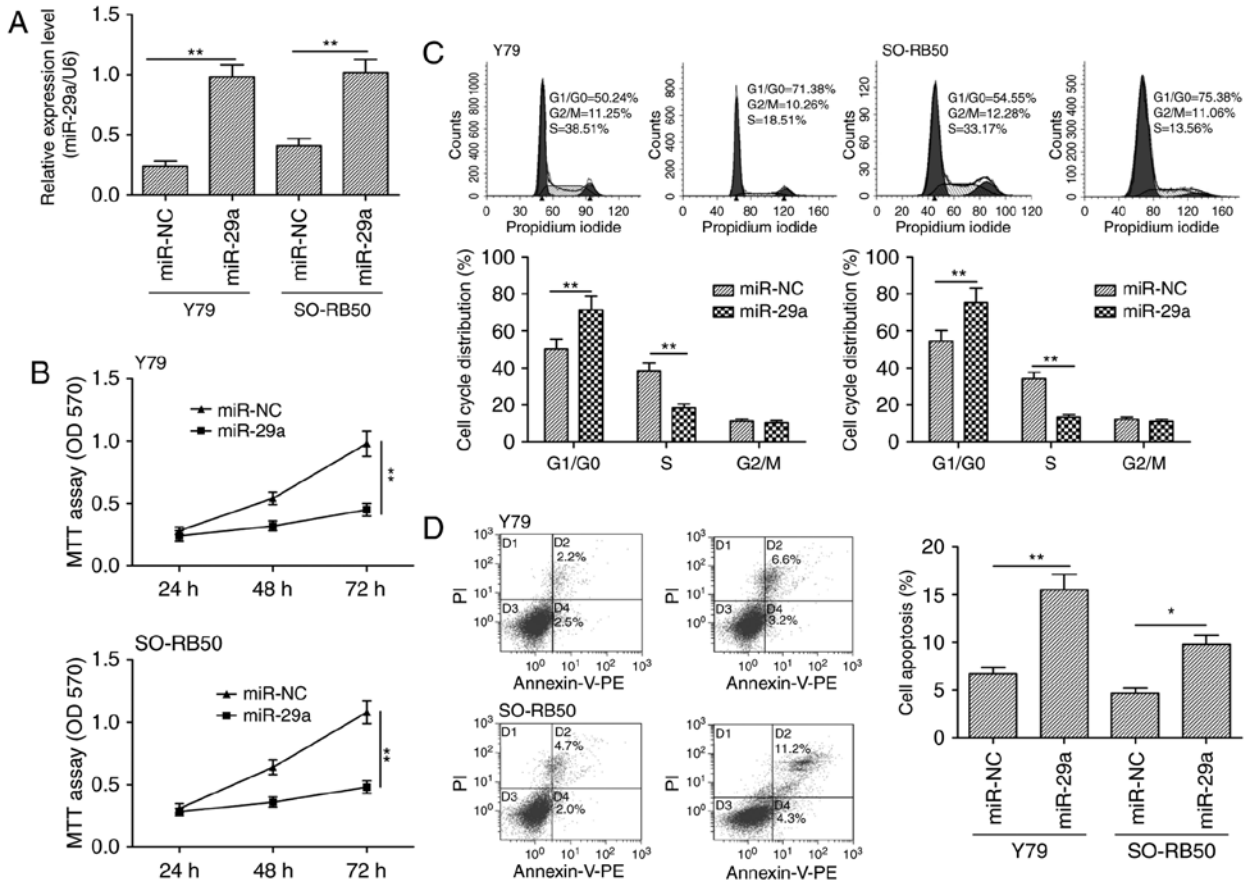

Figure 2. miR-29a inhibits the proliferation and induces the apoptosis of RB cells. (A) miR-29a expression was confirmed to be increased in the miR-29a mimic-transfected cells, compared with those transfected with miR-NC cells, as confirmed by qRT-PCR. (B-D) Cell proliferation, cell cycle distribution and apoptosis were determined in Y79 and SO-RB50 cells transfected with miR-29a or miR-NC. *P<0.05, **P<0.01.

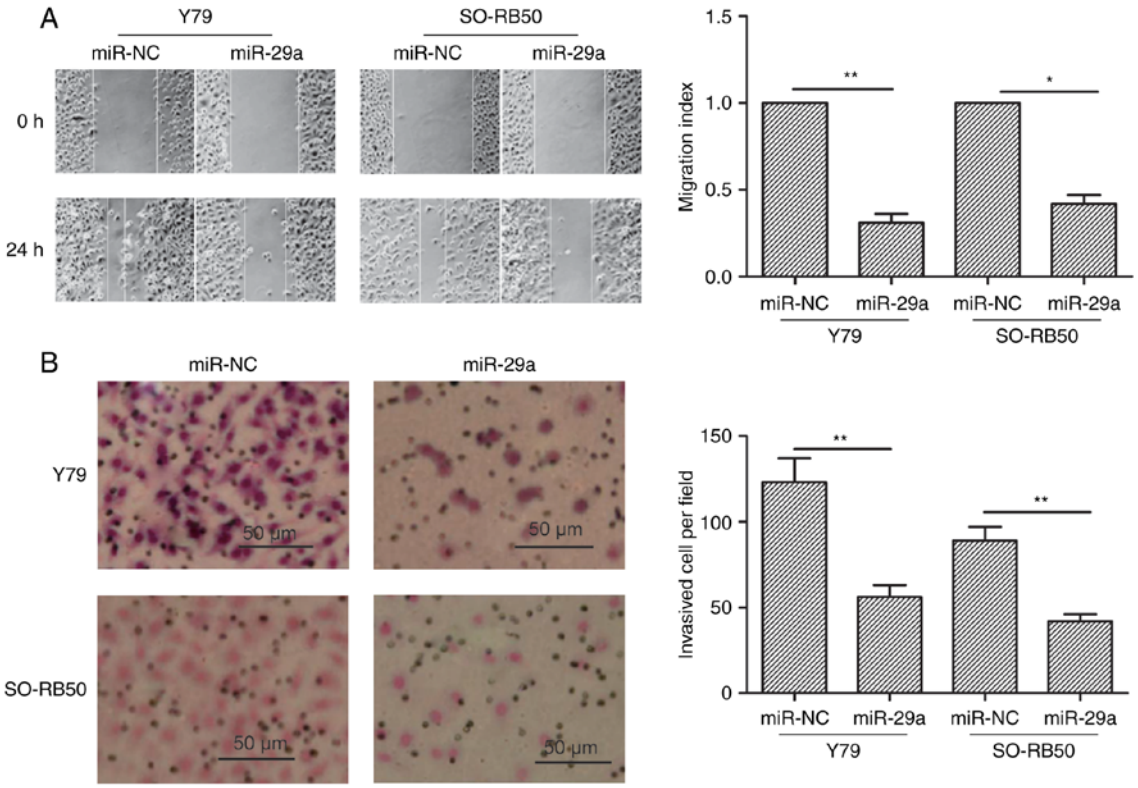

Figure 3. miR-29a inhibits cell migration and invasion of RB cells. (A) miR-29a overexpression inhibited RB cell migration, as determined by wound healing assay. (B) miR-29a overexpression inhibited RB cell invasion, as determined by Transwell invasion assay. *P<0.05, **P<0.01.

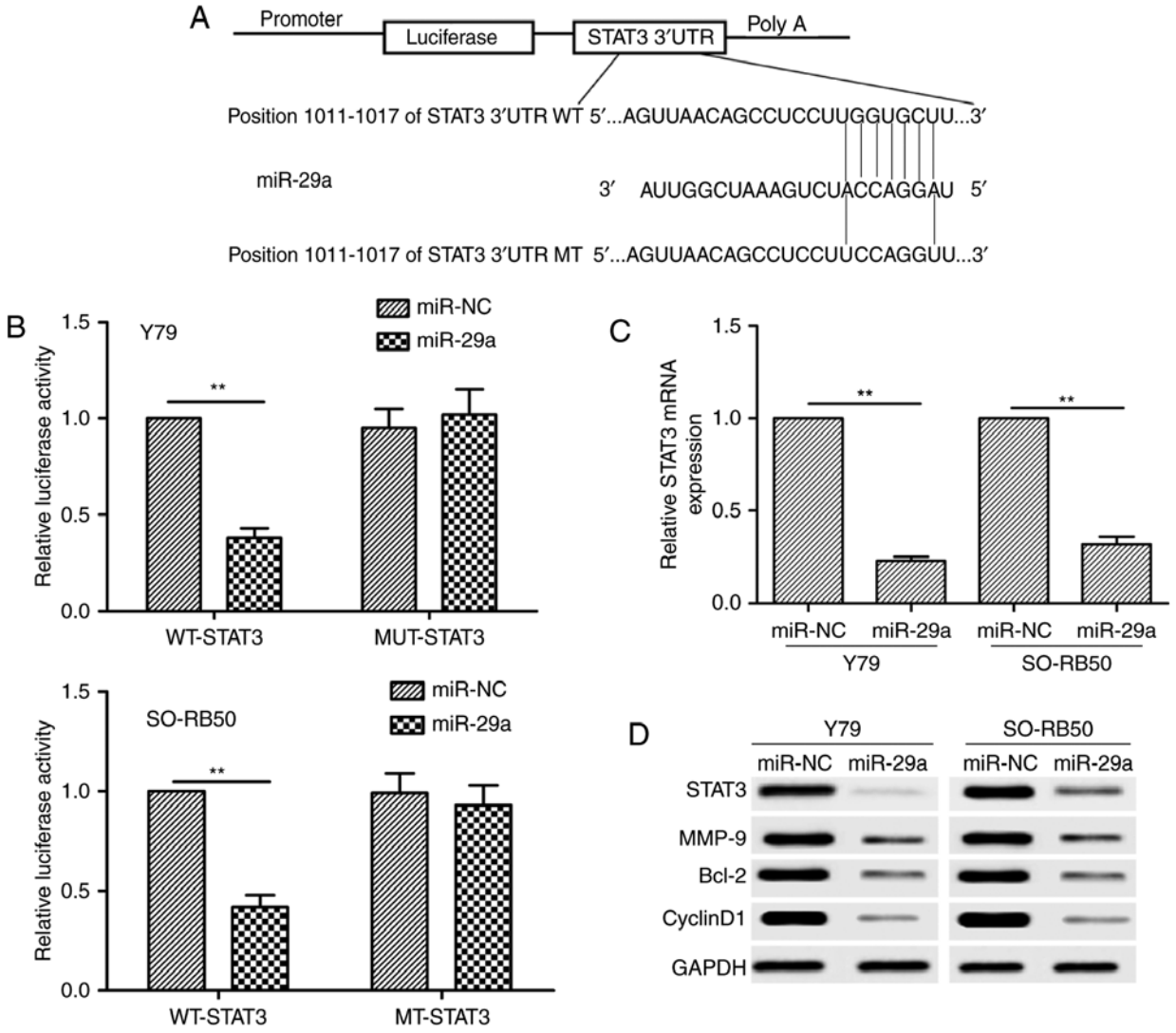

Figure 4. STAT3 is a potential direct target of miR-29a in RB. (A) The predicted binding sites and mutation sites for miR-29a in the 3'UTR of STAT3 are shown. (B) miR-29a overexpression significantly decreased the luciferase activity of the WT-STAT3-3'UTR but not that of the mutant STAT3-3'UTR in Y79 and SO-RB50 cells. (C) Overexpression of miR-29a reduced the *STAT3* mRNA expression levels in Y79 and SO-RB50 cells. GAPDH was used as an internal control. (D) Overexpression of miR-29a reduced the STAT3, cyclin D1, Bcl-2 and MMP-9 protein levels in Y79 and SO-RB50 cells. GAPDH was used as an internal control. $^{**}P<0.01$.

retinal samples by qRT-PCR. We found that RB tissues had a higher expression of *STAT3* mRNA relative to the normal retinal samples (Fig. 5A). In addition, a statistically significant inverse correlation was found between the miR-29a level and STAT3 mRNA level in RB tissues by Spearman's correlation analysis (r=-0.731; P<0.001, Fig. 5B).

STAT3 overexpression reverses the effect of miR-29a on RB cells. To further determine whether *STAT3* is a functional target of miR-29a in RB cells, we performed a rescue experiment involving transfection of STAT3 plasmids (lack of 3'UTR) into miR-29a-expressing RB cells. RB cells transfected with the STAT3-overexpressing plasmid showed restoration of STAT3 expression, which was reduced via miR-29a overexpression (Fig. 6A). Moreover, STAT3 overexpression reversed the effect of miR-29a on cell proliferation, cell cycle, apoptosis, migration and invasion (Fig. 6B-F). Taken together, these results indicated that miR-29a exerts its biological effect in RB by suppression of STAT3.

miR-29a inhibits tumor growth in a mouse model. We assessed the *in vivo* therapeutic efficacy of *miR-29a* in BALB mice. Y79 cells transfected with miR-29a mimic or miR-NC were subcutaneously injected into the flank regions of nude mice. We found that tumor growth was slower in the miR-29a group compared to the miR-NC group (Fig. 7A). On day 35, the mice were sacrificed, tumors were removed and weighed. The tumor size and weight in the miR-29a group were significantly decreased compared to these parameters in the miR-NC group (Fig. 7B and C). We also detected STAT3 protein expression in tumor tissues of nude mice, and found that STAT3 expression was decreased in the miR-29a group (Fig. 7D). Taken together, these data showed that miR-29a inhibits tumorigenicity *in vivo*.

Discussion

It is well documented that various microRNAs are involved in the initiation and development of RB by acting as oncogenes or tumor-suppressor genes (9,10). For example, Liu *et al* reported

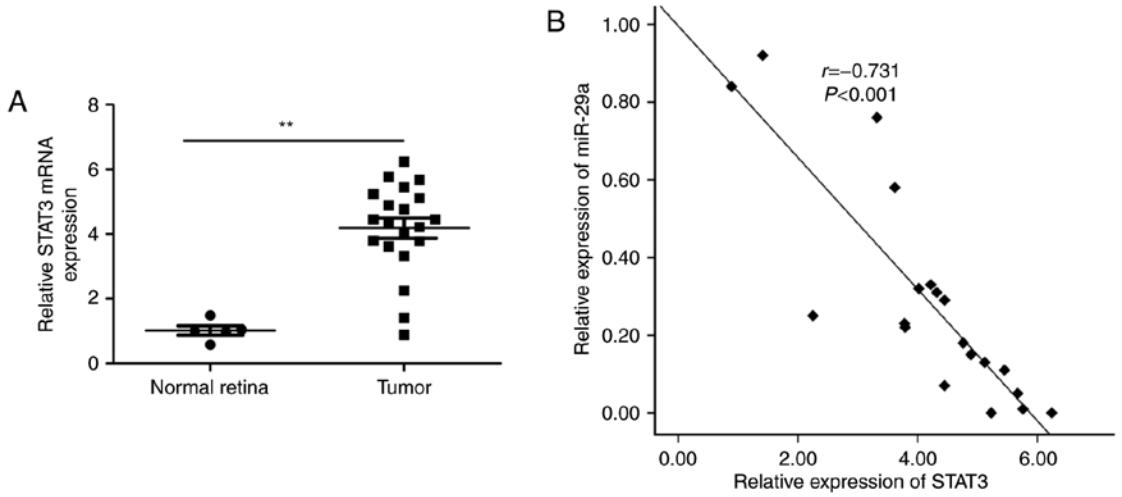

Figure 5. STAT3 expression is upregulated and is inversely correlated with miR-29a expression in RB tissues. (A) Expression of *STAT3* mRNA was found to be upregulated in RB tissues compared to normal retinal tissues. GAPDH was used as an internal control. (B) Inverse relationship between STAT3 and miR-29a expression was noted in the RB tissues by Spearman's correlation analysis. **P<0.01.

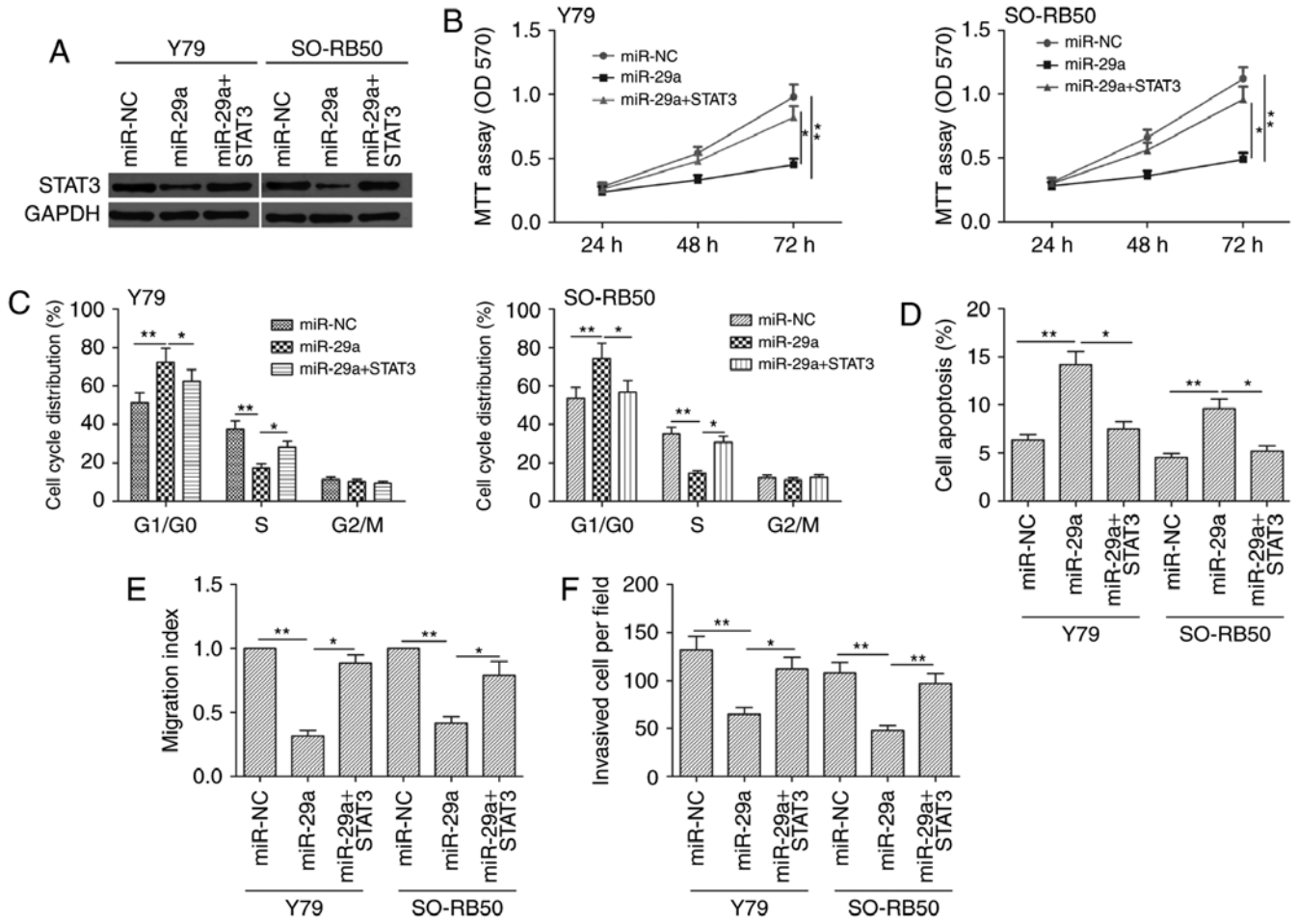

Figure 6. STAT3 overexpression reverses the effect of miR-29a on RB cells. miR-NC mimics, miR-29a mimics or miR-29a mimics plus pcDNA3.1-STAT3 were transfected into Y79 and SO-RB50 cells. (A) STAT3 protein expression was determined in the cells by western blot analysis. GAPDH was used for normalization. (B-F) Cell proliferation, cell cycle distribution, apoptosis, migration and invasion were determined in the cells. *P<0.05, **P<0.01.

that ectopic expression of miR-124 significantly suppressed cell proliferation, colony formation, migration and invasion, induced cell apoptosis in the RB cells by repressing STAT3 (18). Wu *et al* found that enforced expression of miR-204 in RB cells inhibited proliferation and invasion *in vitro* and suppressed tumor growth *in vivo* by targeting cyclin D2 and MMP-9 (19). Martin *et al* demonstrated that overexpression of miR-449a and miR-449b in RB cells significantly impaired proliferation

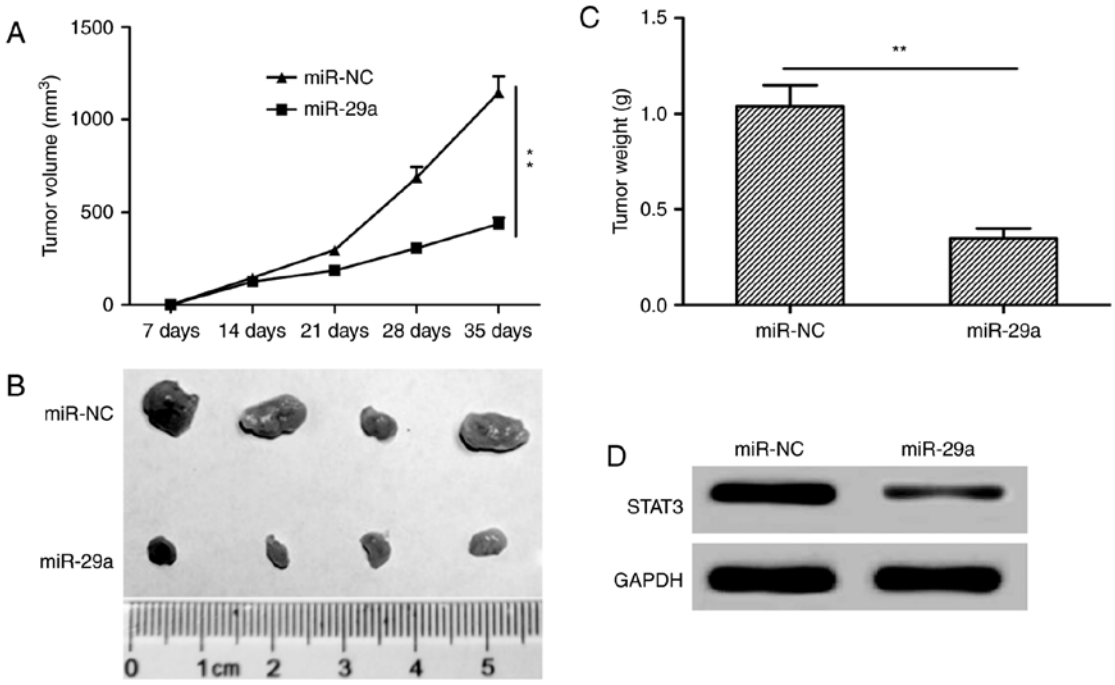

Figure 7. miR-29a inhibits tumor growth in a mouse model. (A) The tumor growth curve was established by measurement of the tumor volume. (B) Tumors were harvested on day 35, and tumor tissues were imaged. (C) Tumors were harvested on day 35, and tumor weight was measured. (D) The STAT3 protein expression was determined in tumor tissues from nude mice. GAPDH was used as an internal control. **P<0.01.

and increased apoptosis of tumor cells (20). Gui *et al* showed that mIR-21 functions as an oncogene in RB via regulation of the PTEN/PI3K/AKT pathway (21). In the present study, we found that RB tissues and cell lines had higher expression of miR-29a compared with that noted in normal retinal tissues. Function assays demonstrated that restoration of miR-29a in RB cells impaired cell proliferation, migration and invasion, and induced cell apoptosis *in vivo*, as well as impaired tumor growth *in vivo*. These results support the conclusion that miR-29a plays a crucial role in RB progression.

miR-29a, located on chromosome 7q32 (22), has been reported in the literature as playing a tumor suppressive role and exerting inhibitory effects on cell proliferation, migration, and invasion in a subset of cancer (12-16). However, the biological function and underlying mechanism of miR-29a in RB have not been explored. Here, our results showed that miR-29a expression in RB specimens was significantly lower than that in normal retinal tissues. Interestingly, the expression of miR-29a in human RB cell lines was also downregulated compared to normal retinal tissues. Subsequently, we found that overexpression of miR-29a in RB cells inhibited cell proliferation and promoted cell apoptosis, as well as decreased the migration and invasion capacity of RB cells *in vitro*. Furthermore, we observed that miR-29a overexpression decreased tumor growth *in vivo*. These results suggested that miR-29a functios as a tumor suppressor in RB.

It is well documented that miRNAs exert their biological function in cancer by regulating expression of their downstream target genes (23). Through three target prediction programs (TargetScan7.1, PicTar and miRDB) putative miR-29a targets were predicted. Our analysis suggests that STAT3 is a potential target of miR-29a. Subsequently, STAT3 was identified as a potential functional target of miR-29a in RB by luciferase assay, qRT-PCR and western blot analysis. STAT3 has been reported to be involved in the development and progression of cancer by regulating cell proliferation, migration, invasion, cell apoptosis and cell cycle arrest (24,25). Importantly, STAT3 exerts its biological role by regulating multiple downstream gene, such as cyclin D1 (cell cycle related gene), survivin, Bcl-xL, Bcl-2 (cell apoptosis-related gene), VEGF, and MMP-2 and MMP-9 (cell invasion-related gene) (24-28). Recently, a study showed that STAT3 expression was upregulated in RB tissues, and that knockdown of STAT3 inhibited cell proliferation *in vitro*, and suppressed tumor growth *in vivo* (28,29). A recently study revealed that STAT3 was regulated by miR-124 in RB (18). In this study, we found that miR-29a overexpression significantly inhibited STAT3 expression and expression of its downstream genes cyclin D1, Bcl-2 and MMP-9. In addition, we found that miR-29a was inversely correlated with *STAT3* mRNA in human RB tissues. Overexpression of STAT3 partially reversed the effects of miR-29a on RB cell proliferation, cell cycle, apoptosis, migration and invasion. Our *in vivo* study also confirmed that miR-29a suppressed tumor growth in nude mice by repressing STAT3. These observations provide the first line of evidence, to the best of our knowledge, that miR-29a exerts it tumor suppressor role in RB via the regulation of STAT3.

In summary, our findings confirmed an inhibitory effect of miR-29a in RB by demonstrating significantly impaired proliferation, migration, invasion and promotion of apoptosis in tumor cells by suppressing STAT3, suggesting that miR-29a could be a potential therapeutic target for RB in the future.

Acknowledgements

The present study was funded bythe Finance Department of Jilin Province (3D5177873429).

References

1. Shields CL and Shields JA: Retinoblastoma management: advances in enucleation, intravenous chemoreduction, and intra-arterial chemotherapy. Curr Opin Ophthalmol 21: 203-212, 2010.
2. Jabbour P, Chalouhi N, Tjoumakaris S, Gonzalez LF, Dumont AS, Chitale R, Rosenwasser R, Bianciotto CG, Shields C: Pearls and pitfalls of intraarterial chemotherapy for retinoblastoma. J Neurosurg Pediatr 10: 175-181, 2012.
3. Kivelä T: The epidemiological challenge of the most frequent eye cancer: Retinoblastoma, an issue of birth and death. Br J Ophthalmol 93: 1129-1131, 2009.
4. Bartel DP: MicroRNAs: Genomics, biogenesis, mechanism, and function. Cell 116: 281-297, 2004.
5. Malan-Müller S, Hemmings SM and Seedat S: Big effects of small RNAs: A review of microRNAs in anxiety. Mol Neurobiol 47: 726-739, 2013.
6. Fabian MR, Sonenberg N and Filipowicz W: Regulation of mRNA translation and stability by microRNAs. Annu Rev Biochem 79: 351-379, 2010.
7. Guo H, Ingolia NT, Weissman JS and Bartel DP: Mammalian microRNAs predominantly act to decrease target mRNA levels. Nature 466: 835-840, 2010.
8. McManus MT: MicroRNAs and cancer. Semin Cancer Biol 13: 253-258, 2003.
9. Yang Y and Mei Q: miRNA signature identification of retinoblastoma and the correlations between differentially expressed miRNAs during retinoblastoma progression. Mol Vis 21: 1307-1317, 2015.
10. Beta M, Venkatesan N, Vasudevan M, Vetrivel U, Khetan V and Krishnakumar S: Identification and insilico analysis of retinoblastoma serum microRNA profile and gene targets towards prediction of novel serum biomarkers. Bioinform Biol Insights 7: 21-34, 2013.
11. Pei YF, Lei Y and Liu XQ: MiR-29a promotes cell proliferation and EMT in breast cancer by targeting ten eleven translocation 1. Biochim Biophys Acta 1862: 2177-2185, 2016.
12. Hu Z, Cui Y, Zhou Y, Zhou K, Qiao X, Li C, Wang S: MicroRNA-29a plays a suppressive role in non-small cell lung cancer cells via targeting LASP1. Onco Targets Ther 9: 6999-7009, 2016.
13. Tang W, Zhu Y, Gao J, Fu J, Liu C, Liu Y, Song C, Zhu S, Leng Y, Wang G, *et al*: MicroRNA-29a promotes colorectal cancer metastasis by regulating matrix metalloproteinase 2 and E-cadherin via KLF4. Br J Cancer 110: 450-458, 2014.
14. He B, Xiao YF, Tang B, Wu YY, Hu CJ, Xie R, Yang X, Yu ST, Dong H, Zhao XY, *et al*: hTERT mediates gastric cancer metastasis partially through the indirect targeting of ITGB1 by microRNA-29a. Sci Rep 6: 21955, 2016.
15. Mahati S, Xiao L, Yang Y, Mao R and Bao Y: miR-29a suppresses growth and migration of hepatocellular carcinoma by regulating CLDN1. Biochem Biophys Res Commun 486: 732-737, 2017.
16. Li R, Liu J, Li Q, Chen G and Yu X: miR-29a suppresses growth and metastasis in papillary thyroid carcinoma by targeting AKT3. Tumour Biol 37: 3987-3996, 2016.
17. Cheng Y, Li Y, Nian Y, Liu D, Dai F and Zhang J: STAT3 is involved in miR-124-mediated suppressive effects on esophageal cancer cells. BMC Cancer 15: 306, 2015.
18. Liu S, Hu C, Wang Y, Shi G, Li Y and Wu H: miR-124 inhibits proliferation and invasion of human retinoblastoma cells by targeting STAT3. Oncol Rep 36: 2398-2404, 2016.
19. Wu X, Zeng Y, Wu S, Zhong J, Wang Y and Xu J: MiR-204, down-regulated in retinoblastoma, regulates proliferation and invasion of human retinoblastoma cells by targeting Cyclin D2 and MMP-9. FEBS Lett 589: 645-650, 2015.
20. Martin A, Jones A, Bryar PJ, Mets M, Weinstein J, Zhang G and Laurie NA: MicroRNAs-449a and -449b exhibit tumor suppressive effects in retinoblastoma. Biochem Biophys Res Commun 440: 599-603, 2013.
21. Gui F, Hong Z, You Z, Wu H and Zhang Y: MiR-21 inhibitor suppressed the progression of retinoblastoma via the modulation of PTEN/PI3K/AKT pathway. Cell Biol Int 40: 1294-1302, 2016.
22. Mott JL, Kurita S, Cazanave SC, Bronk SF, Werneburg NW and Fernandez-Zapico ME: Transcriptional suppression of mir-29b-1/mir-29a promoter by c-Myc, hedgehog, and NF-kappaB. J Cell Biochem 110: 1155-1164, 2010.
23. Catela Ivkovic T, Voss G, Cornella H and Ceder Y: microRNAs as cancer therapeutics: A step closer to clinical application. Cancer Lett 407: 113-122, 2017.
24. Turkson J: STAT proteins as novel targets for cancer drug discovery. Expert Opin Ther Targets 8: 409-422, 2004.
25. Chai EZ, Shanmugam MK, Arfuso F, Dharmarajan A, Wang C, Kumar AP, Samy RP, Lim LH, Wang L, Goh BC, *et al*: Targeting transcription factor STAT3 for cancer prevention and therapy. Pharmacol Ther 162: 86-97, 2016.
26. Masuda M, Suzui M, Yasumatu R, Nakashima T, Kuratomi Y, Azuma K, Tomita K, Komiyama S and Weinstein IB: Constitutive activation of signal transducers and activators of transcription 3 correlates with Cyclin D1 overexpression and may provide a novel prognostic marker in head and neck squamous cell carcinoma. Cancer Res 62: 3351-3355, 2002.
27. Kim BH, Yi EH and Ye SK: Signal transducer and activator of transcription 3 as a therapeutic target for cancer and the tumor microenvironment. Arch Pharm Res 39: 1085-1099, 2016.
28. Cafferkey C and Chau I: Novel STAT 3 inhibitors for treating gastric cancer. Expert Opin Investig Drugs 25: 1023-1031, 2016.
29. Jo DH, Kim JH, Cho CS, Cho YL, Jun HO, Yu Y, Min JK and Kim JH: STAT3 inhibition suppresses proliferation of retinoblastoma through down-regulation of positive feedback loop of STAT3/miR-17-92 clusters. Oncotarget 5: 11513-11525, 2014.